

# Evaluation of absorbed doses in Uranium mine workers using Monte Carlo simulation

## Avaliação das doses absorvidas em trabalhadores de mina de Urânio utilizando simulação Monte Carlo

Leonardo Catusso<sup>1</sup>, Arthur S. B. Z. Alves<sup>1</sup>, Lucio P. Neves<sup>1,2</sup>, Ana P. Perini<sup>1,2</sup>, Carla J. Santos<sup>1</sup>, Lucas M. Silveira<sup>3</sup>, João V. B. Valença<sup>4</sup>, Walmir Belinato<sup>5</sup>, William S. Santos<sup>1,2</sup>.

<sup>1</sup> Universidade Federal de Uberlândia, Programa de Pós-Graduação em Engenharia Biomédica, Uberlândia, Brazil

<sup>2</sup> Instituto de Física, Universidade Federal de Uberlândia, Uberlândia, Brazil

<sup>3</sup> Instituto de Geografia, Universidade Federal de Uberlândia, Uberlândia, Brazil

<sup>4</sup> Grupo de Física Médica Experimental e Computacional, Universidade Federal de Ciências da Saúde de Porto Alegre, Porto Alegre, Brazil

<sup>5</sup> Instituto Federal da Bahia, Vitória da Conquista, Brazil

### Abstract

*The workers of mines, the Cigar Lake mine in Canada, are exposed to naturally occurring radioactive materials. To evaluate the doses to organs in such places, we developed a virtual scenario composed of two virtual anhomomorphic phantoms in a cylindrical mine with several layers of material. The radiation transport was carried out using the MCNPX2.7.0. The results showed that the conversion coefficient for effective dose was 71% higher than the UNSCEAR recommendation, and the most irradiated organs were the thyroid, brain, and esophagus. Furthermore, the female anthropomorphic phantom received the highest doses, given the stature difference compared to the male phantom, thus being positioned closer to the main radiation source.*

**Keywords:** Monte Carlo simulation; occupational dose; Uranium mine; radiological protection; computational anthropomorphic phantom.

### Resumo

Trabalhadores de minas, como a mina Cigar Lake, no Canadá, estão expostos a materiais radioativos de ocorrência natural. Para avaliar as doses em órgãos nesses locais, neste trabalho foi desenvolvido um cenário virtual, composto por dois objetos simuladores antropomórficos virtuais em uma mina cilíndrica, composta por diversas camadas de material. O transporte de radiação foi realizado utilizando o código MCNPX2.7.0. Os resultados mostraram que o coeficiente de conversão para dose efetiva foi 71% superior à recomendação da UNSCEAR, e os órgãos mais irradiados foram a tireoide, cérebro e esôfago. Além disso, o objeto simulador antropomórfico feminino recebeu as maiores doses, dada a diferença de estatura em relação ao simulador masculino, pois estava mais próximo da fonte principal de radiação.

**Palavras-chave:** Simulação Monte Carlo; dose ocupacional; mina de Urânio; proteção radiológica; simulador antropomórfico computacional.

### 1. Introduction

Known as naturally occurring radioactive materials (NORMs), they are elements that are found on Earth and are present mainly in its crust, being products of uranium ( $^{238}\text{U}$ ) and thorium ( $^{232}\text{Th}$ ) radioactive decay chains and the potassium radionuclide ( $^{40}\text{K}$ ) (1). NORMs are present in water, rocks, soil, and air. Referring to their name, they are elements that emit radiation naturally without requiring a stimulus, which is responsible for 86% of the effective radiation dose received by humans (2).

The presence of these radionuclides in the environment is often related to the geological conditions of the region (3). Rocks such as granite, shale, and certain hydrothermal and sedimentary rocks contain higher concentrations of naturally occurring radionuclides (4). Some minerals can influence the concentration of NORMs in these rocks, such as uraninite, carnotite, and autunite for uranium; monazite and thorianite for thorium; sylvan and carnallite for potassium (5). Human activities such as mining can raise radioactivity levels in the Earth's crust by introducing underground ores with natural radionuclides to the Earth's surface. These

radionuclides are chemically released into the environment through various ore extraction and processing processes (6).

There are 14 types of uranium deposits in the world. However, only 6 of them are economically significant: primary (U introduced by magmatic processes) IOCG and intrusive deposits, secondary (U dissolved by fluids and deposited in the reduction phase), lithological unconformity deposits, deposits in sandstones, mineralized limestones and mineralized conglomerates (7). Uranium reserves contain a set of elements that have a significant content of nickel (Ni) and arsenic (As), with smaller amounts of cobalt (Co) and variable concentrations of copper (Cu), vanadium (V), lead (Pb), zinc (Zn), molybdenum (Mo), bismuth (Bi), cesium (Ce) and rare earth. The main uranium minerals are Uraninite, Brannerite, Carnotite, Uranophane, and Autunite.

In this study, the Cigar Lake deposit, located in Canada, was utilized as a reference.

The objective of this study was to evaluate the exposure of workers to natural radiation emitted by materials present inside an underground uranium mine. The radiation transport code MCNPX2.7.0 (8)

was used to simulate the uranium mine to achieve this objective. Within the mine, two virtual adult anthropomorphic reference phantoms (male and female) from the International Commission on Radiological Protection (ICRP) (9) were positioned, each containing numerous organs of dosimetric significance.

## 2. Material and Methods

Uranium mine workers were represented by the reference male and female adult voxel anthropomorphic phantoms from the publication ICRP 110 (9). Some of the most important anthropometric data from these phantoms are presented in Table 1.

**Table 1:** Characteristics of the voxel matrix of anthropomorphic phantoms, male and female, from the reference publication ICRP 110 (ICRP, 2009).

Property	Male	Female
Height (m)	1.73	1.63
Mass (kg)	73.0	60.0
Number of tissue voxels	1.946,375	3.886,020
Slice thickness (voxel height, mm)	8.0	4.84
Voxel in-plane resolution (mm)	2.137	1.775
Voxel volume (mm <sup>3</sup> )	36.54	15.25
Number of columns	254	299
Number of rows	127	137
Number of slices	222	348

Source: The author (2024).

The general approach was to build a model of a realistic occupational exposure scenario of workers inside a uranium mine exposed to naturally occurring radioactivity, in which individuals are standing on the mine floor and monitored by a Geiger-Müller counter. To simplify the exposure scenario, without compromising the results, the mine was considered as a cylinder 15 m long and with a radius of 5.0 m. The volume of the cylinder, which defines the mine, was filled with atmospheric air with a density of 1.2 kg/m<sup>3</sup>, the anthropomorphic phantoms were positioned in the central region and standing on the mine floor.

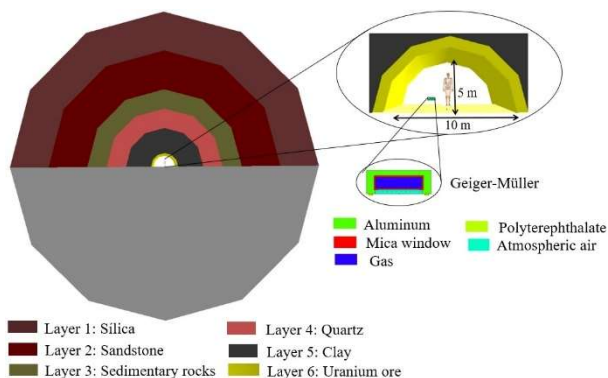


**Figure 1.** View of the main layers of the uranium mine and the anthropomorphic computational phantom inside the hall (out of scale).

The ore body, where mineralization occurs, is located at a depth of approximately 450 m, with five layers above. Figure 1 shows the main compositions of the earth layers that form uranium deposits (10).

The main characteristics of the simulated scenario for each of the layers were: in the quaternary cover, the predominant composition is silica (density 2.65 g/cm<sup>3</sup>); the sandstone layer has a variable composition: 65.58% Oxygen, 32.8% Silicon, 0.87% Aluminum, 0.53% Iron, 0.08% Potassium, and 0.33% other materials (density 2.65 g/cm<sup>3</sup>); the layer of sedimentary rocks is composed of: 65.34% Oxygen, 32.1% Silicon, 0.75% Aluminum, 0.72% Iron, 0.14% Potassium, 0.17% Magnesium; 0.13% Titanium, among other elements with lesser expression; the layer of Quartzite (30 m thick) is composed of: 65.1% Oxygen, 31.6% Silicon, 0.75% Aluminum, 0.72% Iron, 0.14% Potassium, 0.17% Magnesium, 0.13% Titanium, 0.10% Thorium, 0.08% Uranium, 0.16% Lead, among other elements; the fifth layer (Clay), occurs concomitantly with the ore body and the composition is given by: 65.22% Oxygen, 29.2% Silicon, 1.15% Aluminum, 1.02% Iron, 0.74% Potassium, 0.37% Magnesium, 0.33% Titanium, 0.28% Thorium, 0.56% Uranium, 0.19% Lead, 0.12% Potassium, 0.08% Gold, and 0.74% other elements. The sixth layer (density 6.5 g/cm<sup>3</sup>) is the ore body, located 450 m deep, presenting mainly Oxygen, Silicon, Aluminum, and Iron, smaller amounts of Potassium, Magnesium, Titanium, Thorium, and Gold, and, more importantly, 7.00% of uranium (15).

The ground thickness used in the simulation is 10 meters. The distance between the superficial part of layer 6 and the central point of the ground where the anthropomorphic phantom was positioned is 5 meters.

The absorbed doses by the organs and tissues from the phantoms were calculated using the F6 tally (MeV/g/source-particle) of the MCNPX2.7.0 code. These results were normalized by the absorbed dose in air obtained from a Geiger-Müller counter located 1 m above the mine floor. Information on the main materials and geometric model of the counter can be seen in Figure 1.

The NORM source, composed of <sup>238</sup>U and <sup>232</sup>Th decay chains and the <sup>40</sup>K radionuclide, was considered a cylindrical source with a length of 15 m and a radius of 5 m. The source was defined as isotropic and spontaneously emitting the natural radiation present in the layer of earth (Layer 6) that contains the uranium ore and workers. From a computational modeling point of view, using a radius greater than 5 m implied proportionally larger relative errors in the obtained results. To reduce simulation errors to reasonable values (<10%) (8), in all exposure scenarios, one billion particle histories were used.

The equivalent doses (Equation 1) of a set of organs and tissues were determined separately for both genders from the computational anthropomorphic phantoms,

$$H_T = \sum_R w_R \times D_{T,R} \quad (\text{Equation 1})$$

where  $D_{T,R}$  is the absorbed dose in the organ or tissue of interest and  $w_R$  is 1 because it is the radiation weighting factor provided in ICRP publication 103 (11) for photons and electrons.

Once the average equivalent doses by gender have been determined, they are multiplied by the weighting factors for each tissue and added together to determine the effective dose (Equation 2), as recommended in the publication of ICRP 110 (9).

$$E = \sum_R w_T \times \left( \frac{H_T^M + H_T^F}{2} \right) \quad (\text{Equation 2})$$

where  $H_T^M$  and  $H_T^F$  are, respectively, the T-organ equivalent dose of the male and female anthropomorphic phantom and  $w_T$  is the organ or tissue weighting factor.

In this study, dosimetric results are presented in terms of Conversion Factors ( $CF$ ) for equivalent ( $CF(H_T)$ ) and effective ( $CF(E)$ ) doses.  $CF(H_T)$  values were derived for each configuration by taking the ratios between the organ equivalent doses and the absorbed dose in the detector gas volume. Once the equivalent dose values for each organ were known, for both simulators, it was also possible to determine the effective dose and, subsequently, the respective  $CF$  values.

### 3. Results

In Figure 2, it is possible to see a comparison of the  $CF$  values, depending on the type of radionuclide. As presented,  $^{40}\text{K}$  was the radionuclide that most contributed to the increase in exposure of individuals. The total  $CF(H_T)$  and  $CF(E)$ , resulting from the contribution of the three radionuclides, are presented in Table 2.

As shown in Figure 2, the female anthropomorphic phantom was, on average, more exposed than the male phantom. This difference might be related to the height of the female body, being smaller than the male, therefore staying closer to the main radiation source (ground).

### 4. Discussion

As shown in Table 2 and Figure 2, the organs with the highest  $CF(H_T)$  were the thyroid, brain, and esophagus. The tissues with the lowest values found ( $< 0.5$ ) are, respectively, lung, red bone marrow, lymph nodes, kidneys, bone surfaces, and reminder tissues. Among all the organs evaluated, the male phantom's colon showed the most significant difference, around 85% larger than the female one.

The  $CF(H_{pancreas}^F)$  and  $CF(H_{thyroid}^F)$  were 51% and 47% higher than the data from the male phantom.

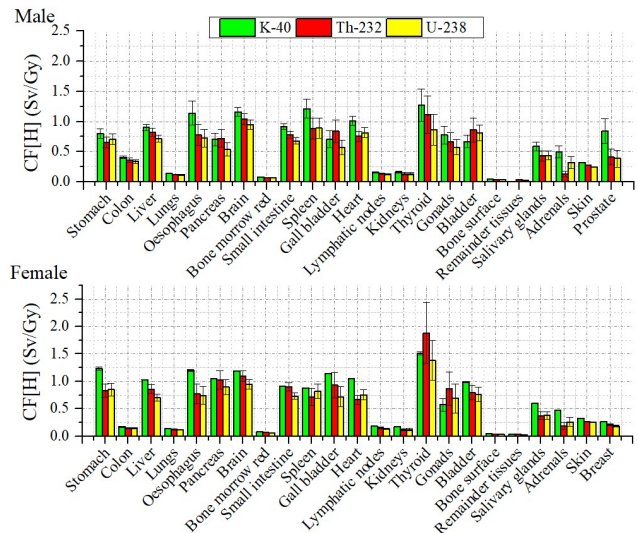


**Figure 2.** CFs for equivalent dose of male and female computational anthropomorphic phantoms. Error bars are related to the statistical uncertainties.

**Table 2.** Conversion factors for equivalent dose, normalized by the absorbed dose in the volume of a Geiger-Müller counter (in Sv/Gy), calculated for professionals inside the uranium mine. In parentheses are the relative percentage errors.

Organs	Male	Female
Stomach	2.16 (0.3)	2.91 (0.4)
Colon	1.11 (0.1)	0.6 (0.1)
Liver	2.44 (0.2)	2.58 (0.2)
Lung	0.38 (0.1)	0.39 (0.1)
Oesophagus	2.64 (0.5)	2.71 (0.5)
Pancreas	1.96 (0.4)	2.97 (0.4)
Brain	3.15 (0.2)	3.23 (0.3)
Red bone marrow	0.21 (0.1)	0.21 (0.1)
Small intestine	2.37 (0.2)	2.54 (0.2)
Spleen	2.98 (0.5)	2.42 (0.4)
Gall bladder	2.12 (0.4)	2.80 (0.7)
Heart	2.58 (0.2)	2.48 (0.3)
lymphatic nodes	0.42 (0.1)	0.47 (0.1)
Kidneys	0.43 (0.1)	0.42 (0.1)
Thyroid	3.24 (0.8)	4.78 (1.2)
Gonads	2.01 (0.4)	2.13 (0.7)
Bladder	2.34 (0.4)	2.54 (0.4)
Bone surface	0.12 (0.1)	0.12 (0.1)
Urethra	1.02 (0.2)	1.30 (0.3)
Remainder tissues	0.10 (0.2)	0.10 (0.2)
Spinal cord	3.02 (0.4)	2.37 (0.4)
Salivary glands	1.45 (0.2)	1.36 (0.2)
Adrenals	0.95 (0.3)	0.92 (0.3)
Skin	0.84 (0.1)	0.85 (0.1)
Prostate	1.64 (0.5)	-
<b>Effective dose</b>		<b>1.2 (0.3)</b>

Source: The author (2024).

The mean  $CF(E)$ , calculated in this study, was 1.2 Sv/Gy. According to the guidelines established by the UNSCEAR (4), the recommended factor for an adult individual is 0.7 Sv/Gy for contaminated soil. Comparatively, the result of this study is around 71% higher than that recommendation. It is important to highlight that this recommendation specifically applies to irradiation geometries arising from natural

radioactivity, such as confined environments, closed spaces, or with few exits.

Table 3 presents the comparison of  $CF(E)$  values provided by the literature involving NORM in different situations and this study. The result of our study is almost twice that of most results in the literature, which were obtained using plane sources distributed in soils.

**Table 3.** Comparison of CFs for effective dose obtained by this study and data from the literature.

Reference	CF[E] (Sv/Gy)
Saito <i>et al.</i> (1998) (12)	0.692
Krstic and Nikezic (2010) (13)	0.491
Pereira <i>et al.</i> (2019) (14)	0.607
<b>This study</b>	<b>1.2 (0.3)</b>

Source: The author (2024).

The study conducted by Pereira *et al.* and Krstic and Nikezic uses the same weighting factors as the present work. However, they only consider the ground surface as the main source of radiation emission. The simulated scenario in this study takes into account both the contribution from the ground and the walls, as already shown in Figure 1. Saito *et al.*'s work used weighting factors predating ICRP 60, and only considered the contribution from the ground as the source. The differences presented in Table 3 may be also related to the anthropomorphic phantoms used, methodology employed to calculate the absorbed dose in the air and the differences in the concentrations of radioactive elements. In addition to that, another important aspect is that previously published works (Table 3) were developed in smaller environments and with fewer emission points.

## 5. Conclusions

The  $CF(E)$  was 71% higher than the UNSCEAR recommendation and almost double the results from the literature. These differences may be related to the calculation methodology used in each paper. The most irradiated organs were the thyroid, brain, and esophagus and the least irradiated were the kidneys, bone surfaces, and remainder tissues. Furthermore, the female anthropomorphic phantom received the highest doses, by its short stature (in comparison to the male phantom), thus being positioned closer to the main source of radiation.

## Acknowledgements

The Conselho Nacional de Desenvolvimento Científico e Tecnológico (CNPq) projects 314520/2020-1 (L.P.N), 312124/2021-0 (A.P.P), 309675/2021-9 (W.S.S), 407493/2021-2 and 403556/2020-1. The Fundação de Amparo à Pesquisa do Estado de Minas Gerais (FAPEMIG) projects APQ-02934-15, APQ-03049-15, APQ-04215-22, APQ-01254-23 and APQ-04348-23. This work is part of the Brazilian Institute of Science and Technology for Nuclear Instrumentation and Applications to Industry and Health (INCT/INAIS), CNPq project 406303/2022-3.

## References

- Ojovan MI, Lee W.E. An Introduction to Nuclear Waste Immobilisation. Elsevier; 2014.
- Filgueiras RA, Silva AX, Ribeiro FCA, Lauria DC, Viglio EP. Baseline, mapping and dose estimation of natural radioactivity in soils of the Brazilian state of Alagoas. *Radiation Physics and Chemistry*. 2020 Feb;167:108332.
- Bezuidenhout J. In situ gamma ray measurements of radionuclides at a disused phosphate mine on the West Coast of South Africa. *J Environ Radioact*. 2015 Dec;150:1–8.
- United Nations. SOURCES AND EFFECTS OF IONIZING RADIATION. 1st ed. Vol. 1. New York: United Nations; 2000. 1–659 p.
- Geraldes MC. Introdução à geocronologia. 7th ed. Vol. 1. Cherna Indústria da Arte Gráfica; 2010. 1–146 p.
- IAEA. IAEA Safety Standards Radiation Protection and Safety of Radiation Sources: International Basic Safety Standards INTERIM EDITION for protecting people and the environment No. GSR Part 3 (Interim) General Safety Requirements Part 3 [Internet]. 2011. Available from: <http://www-ns.iaea.org/standards/>
- OECD Nuclear Energy Agency, International Atomic Energy Agency. Uranium 2014: Resources, Production and Demand. 2014.
- Pelowitz, D. B. (2011). *Mcnpx Tm User' S Manual*. April.
- ICRP. ICRP Publication 110 Adult Reference Computational Phantoms. 2nd ed. Vol. 39. Elsevier; 2009. 1–170 p.
- Pagel M, Ruhlmann F, Bruneton P. The Cigar Lake uranium deposit, Saskatchewan, Canada. *Can J Earth Sci*. 1993 Apr 1;30(4):651–2.
- ICRP. (2007). *International Commission on Radiological Protection: ICRP Publication 103, The 2007 Recommendations of the International Commission on Radiological Protection* (1st ed., Vol. 37). Elsevier.
- Saito K, Petoussi-Hens N, Zankl M. Calculation of the Effective Dose and Its Variation from Environmental Gamma Ray Sources. *Health Phys*. 1998 Jun;74(6):698–706.
- Krstic D, Nikezic D. Calculation of the effective dose from natural radioactivity in soil using MCNP code. *Applied Radiation and Isotopes*. 2010 Apr;68(4–5):946–7.
- Pereira MAM, Silveira LM, Nannini F, Neves LP, Perini AP, Santos CJ, *et al.* Dosimetric evaluation of individuals to 238U series, 232Th series and 40K radionuclides present in Brazilian ornamental rocks using computational simulation. *Ecotoxicol Environ Saf*. 2019 May;173:401–10.
- CAMECO. Cigar Lake Operation Northern Saskatchewan, Canada. National Instrument 43-101. 2016.

## Contact:

Leonardo Catusso  
UFU

Av. João Naves de Ávila, 2121  
38408-100 Uberlândia - MG – Brasil

[leonardo.catusso@ufu.br](mailto:leonardo.catusso@ufu.br)

[leonardo.catusso@pucrs.edu.br](mailto:leonardo.catusso@pucrs.edu.br)